Fall 12-15-2017

Effects of Crude Oil on Tumor Suppressor p53 Polymorphisms in Laboratory-Exposed Atlantic Killifish, Fundulus heteroclitus

Allison Margaret Nadler
Seton Hall University, allison.nadler@student.shu.edu

Effects of Crude Oil on Tumor Suppressor p53 Polymorphisms in Laboratory-Exposed Atlantic Killifish, *Fundulus heteroclitus*

Allison Margaret Nadler

Submitted in partial fulfillment of the requirements for the degree of Master of Science in Microbiology from the Department of Biological Sciences of Seton Hall University

December 15, 2017

Approved by

Acknowledgements

Completion of this master's thesis was possible with the extensive support of a few people that I would like to take the opportunity to recognize.

I am grateful to the professors and staff of the Seton Hall Department of Biology for their wisdom, guidance, and inspiration, which fueled my passion for science, my desire to learn, and my growth both as a student and as a researcher. A special mention goes to my former professors and mentors from my undergraduate Drew University for their contribution to my love for science and periodic correspondence encouraging my continued learning.

Special thanks to my committee members for taking their valuable time to review this project and input their expert advice. I also thank my peers, lab mates, and friends made in the master's program for sharing in the camaraderie, scientific and nonscientific discussions, anxiety, and fun we all had here.

My profound gratitude is extended to my family and close friends for their constant, unwavering support. Without their backing and encouragement I would not have pursued or been able to complete this degree. Their endless belief in my ability, patience on my most frustrating of days, and unconditional love has led me to becoming the student and the person I am today. A special thanks goes to my mom and dad for fostering my love of science and perseverance despite adversity.

Last and most importantly, I would like to extend my sincere thanks to Dr. Carolyn S. Bentivegna, my mentor. Without Dr. B, this thesis and the completion of my master's degree would not have been possible. She welcomed me into her lab late in my academic involvement in the program. She quickly and efficiently taught me the ropes, and took a chance on me to pursue a topic she had been interested in for some time. She gave me the opportunity and encouragement to directly apply techniques I had become familiar with as well as broadening my horizons, teaching me new skills, and taking me out of my comfort zone with presentations and conferences. I will forever be indebted to Dr. B for her patience, guidance, and occasional discussion of our shared love of horses and cats to lighten the mood. I will forever appreciate her unfailing faith, kindness, and will miss her terribly. I hope in all my pursuits I make her proud.

Research funds were provided to Louisiana State University, Seton Hall and Rutgers University by the Louisiana Department of Wildlife and Fisheries (LDWF)-LSU Contract #69670, and to Seton Hall University by the NJ Department of Environmental Protection- SHU Contract # SR11-006. Additional thanks goes to Keith Cooper, Ph.D. at Rutgers University Department of Biochemistry and Microbiology, New Brunswick, NJ, for assistance and use of the aquaculture lab for specimen collection, housing, and dosing. Additional thanks go to the Seton Hall University Department of Biological Sciences for funding under primary investigator Carolyn S. Bentivegna, Ph.D.

Table Of Contents **Page #**

Tables

Figures

Abstract

Polycyclic aromatic hydrocarbons (PAHs), constituents of crude oil, are implicated as a potent source of adverse toxicological effects on living organisms. To model the effects of PAHs in response to environmental oil spill disasters a species of killifish (*Fundulus heteroclitus*) was captured and exposed to crude oil in a laboratory-controlled setting. Over a period of 7 days, fish were dosed with crude oil by gavage, culled, and organs were harvested for analysis. Excitation-emission matrix spectroscopy (EEMS) of gall bladder tissue homogenates was used to verify exposure. Effects of PAHs on the *p53* gene were evaluated as an indicator of genotoxicity. P53 is a tumor suppressor protein that when mutated is implicated in a variety of cancers and genomic instability. Specifically, the *p53* DNA binding domain of the gene was amplified from liver tissue using PCR and analyzed using single-stranded conformational polymorphism (SSCP). SSCP showed that across control and treated killifish, 8 unique genetic profiles could be identified, indicating a combination of native polymorphisms with two unique profiles only seen in Day 7 exposed fish. EEMS analysis on samples from Days 3 and 7 confirmed PAH exposure. Several experimental profiles found in both control and treated fish were cloned and re-subjected to SSCP. Results showed masked polymorphisms in experimental and control fish. Subsequent DNA sequencing of clones showed multiple point nucleotide changes associated with different SSCP profiles. These polymorphisms were found primarily in introns but also exons, where 4 of 6 changes in exposed fish were substitutions of the amino acid asparagine (Asn) for aspartate (Asp). These findings suggest the possible occurrence of crude oil-related mutagenesis in critical gene targets and provide a process for identifying them.

Introduction

British Petroleum's April 2010 *Deepwater Horizon* (DWH) oil spill is one of the most devastating ecological events in recent years during which the Gulf of Mexico and its coastal regions were exposed to approximately 171 million gallons of crude oil (Adams, 2015). The ecological ramifications of this and other oil spills extend from the acute toxicity on the biome to the long term bioaccumulation of the components of crude oil in sediment, sea water, coastal regions, and wildlife where effects are more uncertain. One group of environmentally significant compounds found in crude oil are the polycyclic aromatic hydrocarbons (PAHs) composed of nonpolar, highly lipophilic and petrogenically sourced, multi-ringed substances. PAHs from crude oil spills are monitored using fluorescence analysis of gall bladder bile (Jewett *et. al.*, 2002, Jung *et. al.*, 2011). The different numbers and positions of the fused benzene ring structures generate unique spectra allowing their detection and quantification (Beyer *et. al.*, 2010, Ferretto *et. al.*, 2014). *Fundulus heteroclitus*, commonly called killifish or mummichogs, are small, teleost fish endemic to the estuarine American Atlantic coast, and they have historically shown the ability to adapt and survive in response to environmental contaminants (Duvernell, 2008). Studies following the DWH oil spill show toxicological effects in Gulf killifish (*F. grandis*), including immune system deficiencies (Ali *et. al.*, 2014) and genotoxicity (Whitehead *et. al.*, 2011). In this study, *F. heteroclitus* served as a model organism for investigating mutagenic effects of DWH crude oil, or Macondo 252 (MC252) oil, in a laboratory

setting using fluorescence analysis to detect the presence of PAH-like compounds and polymerase chain reaction followed by single stranded conformational polymorphism analysis to detect possible genotoxicity.

While there are hundreds of known PAHs, sixteen are noted by the United States Environmental Protection Agency (EPA) as linked to adverse effects on humans and the environment (Pampanin and Sydnes, 2013). While not categorized as one of the twelve initial persistent organic pollutants (POPs), crude oil is known to persist in the environment for periods of over ten years (Short *et. al.,* 2003). The lingering of crude oil in the environment, particularly the toxic PAHs, has been established in multiple studies. A 2001 study showed that moderately oiled beaches that resulted from the 1989 *Exxon Valdez* spill in the Gulf of Alaska and along Prince William sound still show PAH deposits in the intertidal zone (Short *et. al.,* 2003), (Irvine *et. al*., 2006).

Killifish, specifically *F. heteroclitus,* are ideal as biosensors for environmental pollutants because they show clinal variation where populations can vary based upon geographic location, and groups have high site fidelity and a narrow home range allowing for genetically homogenous populations (Teo *et. al.,* 2003). They are often the last surviving fish species in highly polluted waters such as the Newark Bay, where the fish display a variety of effects on exposure endpoints such as reproductive disturbances, chemical desensitization, and endocrine disruption (Bugel *et. al.,* 2010). Their common use as a sentinel species has led to a breadth of literature on their reaction to exposure and the subsequent adverse effects, including studies on the effects of the

DWH oil spill on related species *F. grandis* which is the one of the most commonly occurring vertebrate species found in the Gulf of Mexico estuarine marshes (Whitehead *et. al.,* 2011).

Genotoxicity is investigated in this student to determine if there is a link between this adverse effect and exposure to crude oil. As an organism ingests contaminated substances, the kidneys or liver metabolize these fused benzene rings. Metabolism of polycyclic aromatic hydrocarbons occurs primarily via oxidation by the cytochrome P450 family of enzymes. PAH metabolites formed by cytochrome P450 (CYP450) peroxidase yield radical ions or dihydrodiol epoxides, which can cause direct DNA damage through the formation of DNA adducts or oxidative damage by the formation of radical cations, either of which can lead to carcinogenesis (Muñoz and Albores, 2011). However, a second metabolic pathway that involves the formation of PAH-o-quinones by dihydrodiol dehydrogenase is of particular concern because PAH-diol epoxides (PAHDEs) are planar molecules that can be reactive and are able to covalently bind to adenine nucleotides yielding high tumorigenicity (Geacintov *et. al.*, 1997). PAHDEs are also able to amplify reactive oxygen species and the damage they cause to DNA nucleotide bases, particularly via the formation of a structure called 8-Oxo-2'-deoxyguanosine (8-oxo-dG) (Quinn *et. al.,* 2008) (Varansi *et. al.,* 1989). This lesion yields DNA that is not only damaged, but also carcinogenic.

Genotoxicity of crude oil in fish is evidenced by DNA adduct formation in both laboratory evaluations of Atlantic cod (Aas *et. al.*, 2000) and field studies such as after the 1996 oil spill by the *Sea Empress* in Wales (Harvey *et. al.*, 1999). Crude oil genotoxicity has also been linked to the presence of tumors in wild caught and laboratory exposed fish (Arcand-Hoy and Metcalfe, 1999, Bailey *et. al.*, 1996). One study linked the prevalence of liver tumors in an Ohio species of

bottom-feeding brown bullhead fish (*Ameirurus nebulosus*) to levels of sedimentary PAHs in the Black River (Baumann and Harshbarger, 1998). This study was then continued to determine the relationship between PAHs and PAH-like metabolites and their role in tumorigenesis by investigating the formation of adduct structures in liver and skin cells in the brown bullhead fish from several locations in Maryland and Washington D.C. (Pinkney *et. al.,* 2004). Hepatic cytochrome P450 was the primary marker studied and a 50%-68% increase in liver and skin tumors was documented in larger, older fish as sediment PAH levels rose to 15 parts per million (ppm). In Nordic coastal sites, DNA adduct levels were found to be elevated in the gill tissue of mussels in six of a total of eighteen study locations correlated to PAH exposure with a r^2 value of 0.73 (Skarphédinsdóttir *et. al.*, 2007) . Phenanthrene and pyrene exposure, two of the sixteen PAHs noted as most toxic by the EPA, were specifically noted as able to induce the highest levels of DNA adducts seen in gill tissue. Evaluating the effects of PAHs on organism survival, organ function, and genotoxicity is important due to the ubiquitous environmental exposure from pyrogenic and petrogenic sources and key in establishing a complete adverse outcome pathway (AOP) where a linear link between toxicant exposure and a population wide outcome can be used to evaluate risk due to exposure.

In this study, the *p53* gene of *F. heteroclitus* was investigated. The gene *p53* is a critical tumor suppressor gene composed of four domains that function to regulate the cell cycle and halt its progression in the presence of DNA damage. It is responsible for arresting cell proliferation before G1 phase or before mitosis at G2 phase to allow for DNA repair of DNA lesions if the cell is critically damaged (Joerger 2010). It is the hub of many cell-signaling pathways, and is responsible for directing a cell toward apoptosis in the event of a cell having more damage than

the endogenous processes are capable of repairing. One function of wild type *p53* is to activate the small subunit of an enzyme called ribonucleotide reductase (RRM2b), which allows for the regulation of the rate of DNA synthesis via the control of the conversion of deoxyribonucleotides from ribonucleotides (Haupt *et. al.*, 2016). Mutant *p53* is able to up regulate the biosynthesis of nucleotides which aides in the uncontrolled proliferation of cancerous cells. Additionally, activation of *p53* in response to DNA damage is able to trigger transcription of multiple gene targets such as cyclin-dependant kinase inhibitor p21, which is able to disrupt the proper progression of the cell cycle in the G1 phase (Mukherjee *et. al.,* 2004). Overriding the proper G-S checkpoints has the ability to cause genomic instability and increased response to other DNA damaging agents. Disruption to the cell cycle is escalated in response to the PAH benzo-[a]-pyrene, a metabolite of pyrene commonly produced in the liver of organisms. Cogenotoxicity can also be seen in combination exposure to PAHs and heavy metals such as cadmium, sometimes making it difficult to parse apart the specific mechanisms of toxicity. Since multiple environmental pollutants are frequently present, laboratory based studies can help elucidate specific mechanisms of genotoxicity.

P53 is the most mutated gene associated with neoplasm formation and subsequent tumorgenesis, and mutations affecting this gene are seen in more than half of all human malignancies (Freed-Pastor and Prives 2012). *P53* mutations are specifically associated with 96% of ovarian serous carcinomas, 86% of small cell lung cancers, 75% of pancreatic cancers and 54% of invasive breast carcinomas where of these, 86% of mutations to the *p53* gene occur between codons 125 – 300 (Glazko *et. al.*, 2004). This region of the gene codes for a protein, which serves as a multifunctional transcription factor and is implicated in processes such as DNA replication,

transcription, repair, and cell cycle regulation. Loss of transcriptional regulatory function and often associated activation of the oncogene mouse double minute 2 homolog (MDM2), can lead to the elimination of a major negative feedback loop that can allow for an increase in amount of mutant *P53* protein (Kamp *et. al.,* 2016). The core domain called the DNA binding domain occurs from codon 94 – 325 and is considered a highly mutative region, with one study finding it to be the location of 95% of missense mutations in 6 key residues in humans (Bullock and Fersht 2001). This region of the gene was selected for further study due to the overlap in multiple studies finding this domain to be the region containing the majority of hotspots and its importance in the function of the P53 protein (Pavletich *et. al.*, 1993).

This study aimed to expose wild New Jersey killifish to MC252 crude oil in a laboratory setting and analyze DNA polymorphisms in the DNA binding region of the *p53* gene. DNA polymorphisms could be a biomarker for crude oil exposure seen after acute or chronic exposure (Pérez-Cadahía *et. al.*, 2008), or could be indicative of adaptation to persistent environmental contaminants. Another study found mutations in the proto-oncogene K-*ras* in pink salmon (*Oncorhynchus gorbuscha*) embryos following dosing with *Exxon Valdez* crude oil using polymerase chain reaction (PCR) with mismatched 3' primers followed by DNA sequencing (Roy *et. al.*, 1999). In the present study, single-stranded conformational polymorphism of PCR products (PCR-SSCP) was used to detect nucleotide changes in *p53* of liver tissue of adult fish. This study then took a further step by cloning and sequencing various SSCP profiles and found multiple sub-profiles, some containing mutations associated with PAH damage. The presence of PAH exposure was determined using Excitation-Emission Matrix spectroscopy (EEMs). Due to the limited number of samples, this study represents a proof of principle for the PCR-SSCP

approach, which has been studied infrequently, but could provide a similar approach to polymorphic analysis that is quicker than microarrays or restriction fragment length polymorphism analysis. To date, however, no research has been found that shows multiple polymorphic sub-profiles that show unique sequence variations following cloning. This suggests that the approach studied here could show a novel attempt to identify DNA sequence variation in response to toxicant exposure.

Materials and Methods

Specimen Collection and Crude Oil Treatment

Atlantic killifish (*Fundulus heteroclitus*) were collected from Little Sheepshead Creek in Tuckerton, NJ on July 12th, 2013. Fish were captured with permission from The New Jersey Department of Environmental Protection: Division of Fish and Wildlife under Permit #1125, and all vertebrate work done in this study was approved under Protocol #08-025 of The Rutgers University's Institutional Animal Care and Use Committee (IACUC) (Zadlock 2017). Live male and female *F. heteroclitus* individuals were caught using baited minnow traps and isolated from other organisms caught by visual examination of species morphology. Immediately, the fish were transported back to Rutgers University in aerated containers containing collection site water to reduce animal distress. The fish were acclimated to laboratory conditions for two weeks before crude oil exposure.

Individuals in the control and experimental groups were maintained in two different tanks for the duration of the treatment, and fish were dosed by gavage. Control fish were exposed to 25 µl of 100% fish oil obtained directly from DayBrook Fisheries (http://www.daybrook.com/). Fish in the experimental group were exposed to 25 µl of a 50% fish oil and 50% crude oil mixture. The crude oil was Macando 252 (MC252) source oil collected prior to the 2010 Deepwater Horizon accident, as well as from other rigs tapped into the same crude oil source. The 100% fish oil was

produced commercially from Gulf menhaden collected in 2009 and used as a vehicle control as well as a means to reduce gastrointestinal distress from crude oil alone. The 50/50 dosage of the experimental group was selected as a maximal tolerated dose without observation of acute toxicity. Control and experimental groups were dosed for three days consecutively, Day 0 through Day 2, and individuals were culled on Day 0, 1, 3, and 7 as seen in **Table 1**. Sacrifice was accomplished using MS-222 (tricaine methanesulphonate) overdose with subsequent cervical spine dislocation (Zadlock 2017).

Table 1: Experimental timeline of fish oil or crude oil exposure and sample sacrifice for control and experimental groups

Schedule	Day 0	Day 1	Day 2	Day 3	Day 4	Day 5	Day 6	Day 7
Start Time	9:00 AM	9:00 AM	9:00 AM	9:00 AM				9:00 AM
Treatment	Dose	Dose	Dose					
Sacrifices	Day 0	Day 1		Day 3				Day 7

Table 1 shows the dosing schedule for the control and treated killifish. Fish oil control or 50/50 MC252/fish oil treatments were administered in 25 µl aliquots via gavage. Fish were dosed on Day 0, 1, and 2 at 9:00 AM and individuals were sacrificed on Day 0, 1, 3, and 7. Control and experimental samples were obtained only on Day 0, 3, and 7 for the P53 polymorphism study. (Table adapted from Zadlock 2017).

PAH Extraction and Fluorescence Analysis

Control and experimental fish were dissected and the organs were removed and stored at -80°C. Intact gall bladders were individually homogenized in 500 µl of 70% ethanol and an additional 500 µl of 70% ethanol was added to extract any PAHs from the tissue. Samples were vortexed for one minute and centrifuged for 20 min at 13,000 rpm at 4°C to pellet the tissue. The supernatant was removed for fluorescence analysis. All ethanol used in this study was KOPTEC 200 proof (VWR International, King of Prussia, PA, USA). Dilutions made with deionized water were performed with 18 Ohm water from Milli-Q Integral 5 (EMD Millipore Inc., Billerica, MA, USA) (Zadlock 2017).

Sample supernatants were analyzed on a Fluorolog 3 (Horiba Jobin Yvon, Inc., Edison, NJ, USA) in 1mL quartz cuvettes with 1cm excitation path lengths. The wavelengths were established using Sigma-Aldrich® PAH standards 1-hydroxypyrene, lot number MKBD7640V, 9-phenanthrol, lot number BGBB3193V and others (Sigma-Aldrich®, St. Louis, MO, USA) (Pena, 2014). Excitation was from 260-400 nm and emission was from 320-480 nm. Fluorescence intensities were represented in 3D contour maps generated through excitation scans for multiple emission wavelengths. Contour maps were depicted as heat maps and showed photon values labeled counts per second per microamps (CPS/µA), where red indicates high intensity fluorescence and blue indicates low intensity fluorescence. 2D scans were generated using EEMS data by fixing emission at 385 nm and running excitation from 260-380 nm. To normalize fluorescence data for each fish, the fluorescence reading in CPS/ µA was divided by fish mass (g) (Zadlock 2017).

DNA Collection and PCR Analysis

Fish liver genomic DNA isolation was performed using a modified Sigma-Aldrich® TRI Reagent ® protocol (Chomczynski 1993). DNA from fish liver tissue or 70% ethanol homogenates (n=47) were utilized: 26 controls having received fish oil exposure and 21 samples having been exposed to the crude oil mixture and culled on Day 3 or 7. Control fish from Day 0, 3, and 7 and treated fish from Day 3 and 7 were utilized.

Each liver sample or homogenate remaining from previous PAH extraction was homogenized in 1 mL of TRI Reagent ® using either a glass homogenizer or a Tissue Tearor ™ Model 985370 (Vernon Hills, IL, USA). The samples were incubated at room temperature for 5 minutes, 0.2 mL of Sigma-Aldrich® chloroform, anhydrous 99+%, was added, samples were vortexed and incubated at room temperature for 15 minutes. The aqueous layers were removed and 0.3 mL of 100% ethanol was added to precipitate the DNA. The DNA samples were pelleted at 2,000 × *g* for 5 minutes at 2-8°C and washed with 1 mL 0.1M Sigma-Aldrich® trisodium citrate, 10% ethanol solution three times with 30 minute room temperature incubations between each wash. DNA pellets were dissolved in 70% ethanol for 20 minutes, repelleted, and left to air dry. Pellets were then dissolved in 0.3 mL 8mM Sigma-Aldrich® NaOH, centrifuged at 12,000 × *g* for 10 minutes, and buffered with 86 µL 0.1M sterile pH 7.5 HEPES solution (AMRESCO, Solon, OH, USA). Absorbance values were taken for each DNA sample at 260nm and 280nm to check for DNA purity and concentration yields using a DU® 730 Life Science UV/Vis Spectrophotometer (Beckman Coulter Inc., Jersey City, NJ, USA). **Table 4** shows the liver sample IDs, their spectrophotometry data and their calculated DNA purities.

To validate the efficacy of DNA isolation, two of the DNA samples, Day 7 Control fish #3 (7C3) and Day 7 Exposed fish #3 (7E3) were amplified using PCR and *Fundulus* heteroclitus beta-actin housekeeping gene primers. All PCR reactions in this study were composed of 12.5 µL of GeneAmp® Fast PCR 2X Master Mix (Applied Biosystems, Warrington, MA, UK), 8.5 µL Molecular Biology Grade Water (Mediatech, Inc., Manassas, VA, USA), 2 µL of relevant DNA, 1 µL of relevant forward primer and 1 µL of relevant reverse primer. Two reactions of each sample were amplified using 10 µM and 1 µM *F. heteroclitus* specific beta-actin primers developed by Frank J. Zadlock IV to ensure the DNA isolated was viable. PCR reactions were run using a MultiGene™ Thermal Cycler Model TC020A with parameters of 1 minute at 95°C and 45 cycles of 1 minute at 95°C, 1 minute at 60°C, and 1 minute at 72°C, ending in a 72°C hold for 7 minutes (Labnet Inc., Edison, NJ, USA). Samples were then held in the machine at 4°C or stored at -20°C.

These four samples were loaded on a 2% agarose gel made with UltraPure ™ agarose, 0.5X tris-borate EDTA (TBE) buffer diluted from UltraPure ™ 10X TBE stock (Life Technologies™, Grand Island, NY, USA) and 10mg/mL Ethidium Bromide (Invitrogen™, Carlsbad, CA, USA). All subsequent agarose gels were made using the same setup and materials, and 6 µL of each sample was loaded combined with 2 µL of 3X Invitrogen™ TrackIt™ Cyan/Yellow Loading Buffer. Samples were run alongside Invitrogen™ 100 bp DNA ladder with 2 µL of 0.5 µg/ µL ladder combined with 2 µL of loading buffer.

Primer Design and Verification

Primers for the *p53* DNA binding domain were designed from National Center for Biotechnology Information (NCBI) Genbank's *Fundulus heteroclitus* tumor protein p53 (tp53),

transcript variant X3, mRNA (Accession XM_012874738.1) using primer3plus (Benson 2005), (Untergasser 2012). The *p53* DNA binding domain location oriented at 845-972 base pairs of the P53 protein was verified using European Molecular Biology Laboratory-The European Bioinformatics Institute (EMBL-EBI) pfam service to align NCBI FASTA nucleotide sequence to the amino acid sequence of the functional domain of the protein showing 141-332 amino acid sequence alignment match (Finn 2016).

The forward primer selected started at base pair 811 and the reverse primer started at base pair 1015 allowing for a 205 base pair amplicon. The oligonucleotide sequences were then run through Integrated DNA Technologies (IDT) OligoAnalyzer® 3.1 Tool to check for minimal self-dimerization, hairpin, and heterodimerization activity (http://www.idtdna.com/Scitools.). A second set of primers for a similar sequence were designed, but not used. **Table 2** below shows the primer design and intended amplicon. A second set of primers was designed but not used.

Table 2: Fundulus heteroclitus p53 DNA binding domain primer design and amplicon

Primer Direction	Melting Temperature (Tm)	Start Location	Oligonucleotide Size (bp)	Sequence
Forward	59.9°C	811	20	5'-CGGAGATGACCACCATTCTT-3'
Reverse	60.1°C	1016	20	5'-TTGCTGTCGCTTTTCTCCTT-3'

Sequence	751	AAGACCCGTA	CACCAAAAGG	CAGAGTGTCA	CCGTGCCGTA	TGAGCGGCCA
	801	CAGCTGGGCT	**CGGAGATGAC**	**CACCATTCTT**	CTCAGCTTCA	TGTGCAACAG
	851	CTCCTGCATG	GGGGGCATGA	ATCGTAGGCC	TATCCTCACC	ATCCTGACCC
205bp	901	TGGAGACACC	AGAGGGGTTG	GTTTTGGGCC	GCAGATGCTT	CGAGGTCCGT
	951	GTCTGTGCCT	GTCCAGGCAG	GGACCGGAAG	ACCGAGGAAG	ACAAC**AAGGA**
	1001	**GAAAAGCGAC**	**AGCAA**GCAAA	AAAAAAAGCG	AAAGAGCGCT	CCTACTCCAG

Table 2 shows the forward and reverse *F. heteroclitus p53* DNA binding domain specific oligo sequences and their associated size, starting base pair number, and ideal melting temperature. The p53 DNA binding domain sequence accessed from NCBI A *Fundulus heteroclitus* tumor protein p53 (tp53), transcript variant X3, mRNA Accession XM_012874738.1 is also displayed with the full gene region highlighted in green. The oligo binding location is shown bracketed on either side of the intended amplicon with the forward primer highlighted in red and the reverse primer highlighted in blue.

PCR reactions were set up as described previously using the *p53* DNA binding domain primer set with run parameters of 2 minutes at 95°C and 35 cycles of 1 minute at 95°C, 1 minute at 60°C, and 1 minute at 72°C, ending in a 72°C hold for 7 minutes. All subsequent PCR reactions were run with these parameters, and successful amplification was confirmed using the gel electrophoresis protocol described above.

To evaluate successful amplification of the desired sequence, fresh PCR samples of Day 0 control fish #8 (0C8) and Day 7 exposed fish #3 (7E3) underwent plasmid preparation using TOPO® TA Cloning Kit for Sequencing using the Invitrogen™ protocol (Abdel-Banat 2002). The cloning reaction was composed of 2.5 µL PCR sample, 1 µL of 1.2 mM NaCl, 10 mM $MgCl_2$, 1.5 µL water, and 1 µL TOPO® vector, and was incubated on ice for 15 minutes. A 2 µL aliquot of the plasmid vector reaction was added to the One Shot ® TOP10 F' Chemically Competent *Escherichia coli* cells, and the mixture was heat shocked at 42°C. A 250 µL aliquot of room temperature super optimal broth with catabolite repression (SOC) media was added to the cells, and the cells were incubated while shaking at 37°C for 1 hour. Competent cells were spread onto pre-warmed 100 µg/mL LB/ampicillin plates that had been treated with 80 µL of 20 mg/mL Thermo Scientific X-Gal and 40 µL of 20 µg/mL Thermo Scientific IPTG (isopropyl β-D-1-thiogalactopyranoside). All subsequent cloning in this study followed this same procedure (Thermo Fisher Scientific, Waltham, MA USA). Cloning reaction plates were incubated overnight at 37°C.

Three white, successfully transformed colonies were selected from each cloning plate using blue-white selection, and suspended in 50 µL Molecular Biology Grade Water (Thermo Fisher

Scientific, Waltham, MA USA). PCR was used to re-isolate the gene of interest using the gene specific p53 forward primer and the plasmid specific M13 kit reverse primer. The samples were run on a gel to ensure successful PCR, and one of each sample (0C8 and 7E3) was sent for sequencing to GenScript DNA Sequencing Service to validate the amplification of the *p53* binding domain (GenScripts Biotech Corporation, Piscataway, NJ).

Polymorphism Analysis using SSCP

Once the primers were validated, PCR gene amplification of the *p53* DNA binding domain was performed on all 47 DNA samples. All PCR samples were run on agarose gels to ensure successful amplification with expected band lengths consistent with 205 base pairs.

Individual 6 µL samples of each PCR reaction were then denatured at 95^{o}C for 10 minutes in 12 µL of formamide loading dye buffer (Invitrogen, Vilinius, LI), and then flash frozen on dry ice. The samples were loaded into 15 well upright BIO-RAD Mini-PROTEAN® TBE Precast Gels that had been rinsed and pre run in 0.5X TBE for 45 minutes at 200 volts. Aliquots (8 µL) of samples were then run at 72 volts for 3 hours with the gel apparatus submerged in ice. Once the tracking dye had run to the bottom of the plastic casing, the gel was cracked open, removed, and soaked in 100 mL of deionized water until the dye had dissipated from the gel or for 20 minutes, and the water was decanted. SYBR® Gold Nucleic Acid Gel stain was diluted from 10,000x to 1x with 1 µL of stain into 50 mL deionized water, and poured over the gel. The gel was covered with aluminum foil and rocked for 30 minutes. The gel was visualized on a UV transilluminator and SSCP variants were recorded (Orita 1989).

Cloning, Sequencing, and Alignment of Polymorphic Profiles

One PCR sample (7E2) was cloned into One Shot ® TOP10 F' Chemically Competent *Escherichia coli* to evaluate amplicon sequence consensus among multiple clones of the same SSCP variant. Fifteen successfully cloned colonies were selected and amplified using PCR and the gene specific primer set. The 15 clones were denatured in formamide buffer and run again on a 15 well upright BIO-RAD Mini-PROTEAN® TBE Precast Gel using the setup as before. The gel was visualized on a UV transilluminator and SSCP variations from the original parent profile were recorded. From the 15 clones, three were selected to sequence, one clone with an SSCP profile similar to the original PCR SSCP profile and two clones with unique or differing profiles.

The above cloning, colony selection, and SSCP evaluation was repeated for two other experimental PCR samples (7E5 and 7E14) and for three control PCR samples (0C2, 3C7, and 7C4) to evaluate two other unique SSCP profiles and comparative clone SSCP profiles. Three clones were selected from each of the two additional experimental sets, and six clones were selected from the three control clone sets to send out for sequencing.

The selected clones were submitted to a sequencing company (GenScripts Biotech Corporation, Piscataway, NJ). Clone sequences were aligned using NCBI Nucleotide BLAST® (Altschul 1990) in order to determine the presence or absence of sequence variants.

This process was repeated for PCR samples 7E5 and 7E14 to evaluate two other unique SSCP profiles from *p53* DNA exposed to crude oil treatment. PCR samples 0C2, 3C7, and 7C4 also were cloned with 15 colonies from each amplification to compare control sample sequences to

the sequences of treated samples. Three clones from each of the experimental clone sets were sent out for sequencing, then aligned and evaluated for sequence variants between like clones. One replicate from each of the control clone sets (three total) were sent out for sequencing to allow for comparative alignment between the control sequence and the experimental sequences above.

Consensus sequences were aligned for clones from the same fish and matched with sequence similar to control clones. Consensus sequences were then translated to the expected amino acid sequence and amino acid variation was determined.

Results

Exposure to PAH-like compounds was determined in gall bladders using EEMS. **Figure 1** shows four representative fish spectra obtained from 3D EEMS of gallbladder homogenates. Control fish from both Day 3 and Day 7 show spectra signatures consistent with the protein albumin, with no strong signal from PAH-like compounds (Zadlock 2017). Day 3 experimental fish #9 (3E9) showed maximal fluorescence at Ex340/Em380-400, which was consistent with the presence of 1-hydroxypyrene. Day 7 experimental fish #2 (7E2) showed maximal fluorescence at Ex260/Em370-380, which was consistent with the presence of 9-phenanthrol, and indicated preferential metabolism of 1-hydroxypyrene-like PAHs. PAH standards for 1-hydroxypyrene and 9-phenanthrol are provided to display predominant PAHs likely present in homogenate tissue, as indicated by similar spectra. **Figure 2** shows the response of all Day 7 fish in 2D spectra. The emission was held at 385 nm, and excitation varied from 260 to 380 nm. Control fish showed 100x less fluorescence than experimental fish. Fluorescence intensity was normalized using fish weight. Spectra confirmed exposure to PAH-like compounds in crude oil of gavaged fish. **Table 3** provides average length and mass measurements for control and experimental fish from all days. Day 1 fish were not processed in this study, but a T-test noted significant size difference in control versus experimental fish was observed.

Figure 1: Representative EEMS of gall bladders of crude oil exposed or control killifish collected on Day 3 or Day 7. Top images indicate spectra for Day 3 control fish #7 (3C7, left) and Day 7 control fish #4 (7C4, right). Middle images indicate spectra for Day 3 experimental fish #9 (3E9, left) and Day 7 experimental fish #2 (7E2, right). Bottom images are PAH standards for 1-hydroxypyrene (0.02 µg/ml, left) and 9-phenanthrol (0.3 µg/ml, right) included for comparison. The fluorescence spectra seen in controls are similar to that of albumin.

Figure 2: Levels of fluorescence (CPS/µA/g) in gall bladders after Day 7 exposure to crude oil or control. This is a graphic representation of fluorescence from 2D EEMS where emission was held at 385 nm and excitation ranged from 260 to 380 nm. Day 7 control (bottom) and experimental (top) fish are compared with each line denoting an individual. Note that the scale for control is 1000x less than for exposure. The gall bladder for Day 7 experimental fish #14 was lost during processing.

Table 3: Average monomorphic measurements of length and mass for male and female control and experimental group fish

	Day 0		Day 1		Day 3		Day 7	
Group	Length (mm)	Mass (g)	Length (mm)	Mass (g)	Length (mm)	Mass (g)	Length (mm)	Mass (g)
Control	68 (9.0)	5.00 (2.1)	67.3 (4.4)	3.94 (0.9)	69.1 (2.8)	4.74 (0.8)	64.9 (3.9)	3.48 (0.7)
Exposed			75.6 (4.4)*	5.75 (1.0)*	74.9 (7.9)*	5.6 (1.9)	72.2 (10.1)*	5.05 (2.6)*

Table 3 indicates the length and mass measurements averaged for all the fish in the study where there was a T-Test significant difference between CON vs EXP group, $p \leq 0.05$; SD (95%) is in parentheses and designated with an asterisks.

Polymorphisms in the DNA binding domain of *p53* were investigated using PCR followed by SSCP. Primers displayed in **Table 2** amplified a single band of 260 bp from genomic DNA of 47 fish, 26 control and 21 experimental. Fish were dosed with crude oil on Day 0, 1, and 2 and control and exposed specimens were culled on Day 0, 3, and 7 to evaluate polymorphisms following acute exposure. Since the liver is a major site of PAH metabolism into active metabolites that show genotoxicity, liver tissue was analyzed. Liver tissue DNA, homogenized and isolated using TRI Reagent ® showed some inconsistency in purity across the 47 sample, as seen in **Table 4** below. Some samples (all controls) required DNA isolated from a previously homogenized pellet that had been frozen, while all experimental livers were homogenized the day of DNA isolation. Initial PCR reactions were all set up using the DNA concentration yields that allowed for calculation of optimal template DNA concentration. Each fish evaluated was given an identifier where the day, group, and fish number were represented as day, experimental group (Control/Experimental), and fish #. For example, fish number 1 from the Day 0 control group was labeled 0C1. Fish are abbreviated this way in text as well as in all figures, tables, and sequences.

Table 4: Killifish liver sample IDs, tissue sample, and spectrophotometry data

Sample ID	Day C/E	A260 n.m.	A280 n.m.	Purity	Concentration (µg/mL)
0C1	0 Control	0.362	0.221	1.64	181
0C2	0 Control	0.694	0.416	1.67	347
0C3	0 Control	0.291	0.183	1.59	146
0C4	0 Control	1.741	1.022	1.70	871
0C5	0 Control	0.878	0.518	1.69	439
0C7	0 Control	0.774	0.475	1.63	387
0C8	0 Control	0.192	0.140	1.37	960
0C9	0 Control	0.143	0.088	1.63	72
0C10	0 Control	0.153	0.094	1.63	77
3C1	3 Control	0.786	0.527	1.49	393
3C2	3 Control	0.989	0.658	1.50	495
3C5	3 Control	0.740	0.489	1.51	370
3C6	3 Control	0.861	0.547	1.57	431
3C7	3 Control	2.695	1.886	1.43	1348
3C8	3 Control	1.414	0.870	1.63	707
3C9	3 Control	0.420	0.268	1.57	210
3C10	3 Control	0.541	0.340	1.59	271
3E1	3 Experimental	0.078	0.051	1.53	390
3E2	3 Experimental	0.046	0.031	1.48	230
3E3	3 Experimental	0.255	0.161	1.58	1275
3E4	3 Experimental	0.173	0.110	1.57	865
3E5	3 Experimental	0.106	0.060	1.77	53
3E6	3 Experimental	0.019	0.007	2.71	95
3E7	3 Experimental	0.220	0.131	1.68	1100
7C3	7 Control	0.178	0.072	2.47	89
7C4	7 Control	0.044	0.024	1.83	22
7C5	7 Control	0.152	0.095	1.60	76
7C6	7 Control	1.152	0.693	1.66	576
7C7	7 Control	0.087	0.055	1.58	44
7C8	7 Control	0.053	0.034	1.56	27
7C9	7 Control	0.037	0.024	1.54	19
7C10	7 Control	0.022	0.016	1.38	11
7C11	7 Control	0.068	0.044	1.55	34
7E1	7 Experimental	0.091	0.047	1.94	46
7E2	7 Experimental	0.269	0.175	1.54	135
7E3	7 Experimental	1.764	1.015	1.74	882
7E4	7 Experimental	0.026	0.015	1.73	13
7E5	7 Experimental	0.030	0.019	1.58	15
7E6	7 Experimental	0.073	0.036	2.03	37
7E7	7 Experimental	0.166	0.107	1.55	83
7E8	7 Experimental	0.228	0.116	1.97	114
7E9	7 Experimental	0.237	0.153	1.55	119
7E10	7 Experimental	0.116	0.069	1.68	58
7E11	7 Experimental	0.193	0.123	1.57	97
7E12	7 Experimental	0.113	0.073	1.55	57
7E13	7 Experimental	0.117	0.075	1.56	59
7E14	7 Experimental	0.042	0.027	1.56	21

Table 4 shows the full list of 47 liver DNA samples, their sample ID, and their spectrophotometry data. A DU® 730 Life Science UV/Vis Spectrophotometer was used to evaluate the A260 and A280 values, and purity was calculated using the standard equation of purity = (A260/A280) where pure, uncontaminated double stranded DNA will have a purity of 1.8 (Glasel 1995). Concentration was derived from the equation dsDNA = (50 µg/mL x $O.D._{260}$ x dilution factor) (Barbas 2001).

The success of the DNA isolations was verified by amplifying two Day 7 samples (7C3 and 7E3) using primers specific to the *Fundulus heteroclitus* housekeeping gene beta-actin at two different concentrations. **Figure 3** shows strong bands present for beta-actin in both samples at approximately 150 base pairs, which is consistent with the expected size of this amplicon (Zadlock 2017). **Figure 4** shows the same two samples amplified with the designed *p53* primers with the beta-actin gene as a comparison. Primer set #1 was selected for continued study. Two DNA samples were amplified using primer set #1 and sent out to GenScripts for sequence verification. Sample 0C8 showed 100% hit identity with the GenBank sequence used to design the primers and sample 7E3 showed 96% identity, confirming the intended amplicon for the primers.

Figure 3: Verification of killifish liver DNA integrity using two concentrations of Fundulus heteroclitus beta-actin primers. Bands at approximately 150 bp were indicative of successful amplification of this gene. 10µM and 1µM concentrations were used to determine ideal primer concentration in further PCR reactions.

Figure 4: Evaluation of designed p53 primer sets 1 and 2 compared with housekeeping gene primers. Primer set #1 was selected for use as it shared an annealing temperature of 60^{o}C with the beta-actin primers. Primer set #2 required an annealing temperature of 63^{o}C and was not utilized. 1µM concentrations of all primers were used in these PCR reactions.

Primer set #1 showed successful amplification of the intended gene, so all DNA samples underwent PCR, gel analysis, and then SSCP. **Figure 3** shows the PCR amplification bands from all 47 fish with the SSCP profiles below. The intended amplicon was 205 bp as the primers were designed from an RNA transcript; however, the actual amplicon was 260 bp indicating additional bases from an intron, which was later confirmed by sequencing.

Figure 5: DNA gel electrophoresis and single stranded conformational polymorphism profiles for control samples and exposed samples. Singular white bands on a black background in each lane showed successful amplification of the gene. SSCP polymorphic profiles are shown as multiple bandings of black on white. Summary assignments (P1-P8) of each SSCP profile are provided in **Table 5**.

Comparison of gels identified eight individual SSCP profiles that were named in order to determine abundance of each variation specific to this study. **Table 5** shows the unique profiles and their abundance where profiles are named P1-P8. Some of the profiles had similar characteristics, such as P1, P3, P5, and P7, which all showed two bands. The variations between them arose in band intensity and relative size of the bands as well as distance of the bands from each other. Slight differences in SSCP profiles have been established to show nucleotide changes that could be significant when sequenced. The profiles in both the control and the experimental fish were varied; however, there was a greater abundance of P1, P2, and P3 across all groups, and these were considered dominant profiles for this population of killifish. Since the fish were all collected from the same site at the same time, and were likely to be from the same school, the variation of profiles in the control were striking. The exposed fish did show the dominant profiles as well as two profiles (P5 and P6) with lower abundance than control examples. Two profiles (P7 and P8) were unique to Day 7 experimental fish and were therefore targeted for DNA sequencing.

Table 5: Summary of SSCP variant profiles

Table 5 shows variation of observed SSCP profiles and provides the number of each profile seen categorized by day and test group. Profile number was assigned arbitrarily and the abundance was not analyzed statistically or considered significant past raw observation.

Eight total profiles were established from the 47 specimens collected, and 6 specimens were investigated further to determine if SSCP profile variations could be connected to polymorphisms within the amplified region of the *p53* gene. The rationale for fish selection was as follows. Experimental fish, 7E2, and control fish, 0C2, shared a similar profile, P1. Comparing them allowed assessment of clone variability from fish with the same original SSCP profile. Experimental fish 7E5 (P7) and 7E14 (P8), and control fish 3C7 (P6) and 7C4 (2), had unique profiles from one another but common profiles in terms of representing their treatment group. Comparing them allowed assessment of nucleotide differences between control and experimental fish.

PCR-SSCP profiles of clones for the six selected fish are shown in **Figure 6**. Profiles of selected controls showed uniformity across 15 randomly selected clones of each fish. Across all 45 clones from the three control fish, only 4 were unique: 0C2(3), 3C7(2), 7C4(2) and 7C4(8). However, clones of experimental fish showed more variability. Clones of 7E2 and 7E5 had three profiles each- 7E2(2), 7E2(7) and 7E2(10) and 7E5(5), 7E5(8) and 7E5(11), respectively. Clone profiles 7E2(2) and 7E5(5) had the dominant profile for their respective fish, and it was most similar to the original PCR-SSCP profile. Clones of 7E14 also showed three profiles, 7E14(4), 7E14(5) and 7E14(12). None of these profiles completely resembled the original PCR-SSCP profile.

Figure 6: SSCP comparisons between original parent sequence and fifteen clones. PCR amplicons from 6 fish were selected for cloning based on their SSCP profiles. Then 15 randomly selected clones per fish were subjected to SSCP. The figure provides the fish designation, original SSCP profile, and the profile of each of its clones. Boxed profiles were selected for DNA sequencing.

Boxed profiles from **Figure 6** were sequenced and aligned to *F. heteroclitus* tumor protein *p53* (*tp53*), transcript variant X3, mRNA (Accession XM_012874738.1) using NCBI BLAST®. Clones of 7E2 were aligned to each other and 0C2(3), which was the control with the highest % identity to 7E2(2), 99% (**Figure 7**). The sequences were 354-355 bp, including an intron of 148 bp. Alignments showed no nucleotide differences within exons. Nucleotide changes occurred at 4 positions within introns.

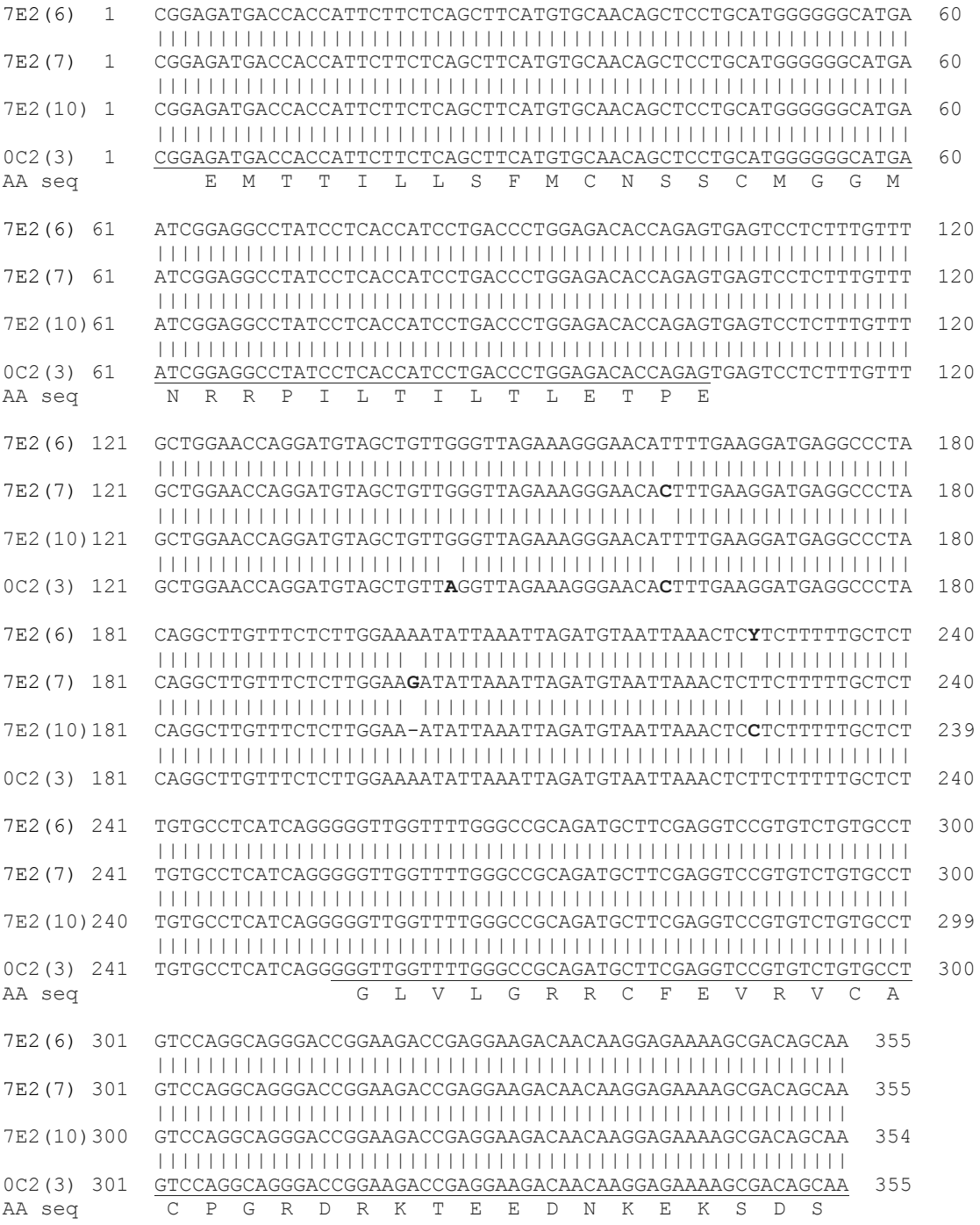

Figure 7: DNA sequences of clones from experimental fish 7E2 and control fish 0C2. Sequences are labeled as day of collection – 7 or 0, treatment – E (experimental) or C (Control), fish number – 2 or 2, and clone (number). Variations in nucleotide sequences are boldfaced and the exons are underlined. The amino acid sequence (AA seq) is based on consensus codons.

Clones of 7E5 were aligned to each other and 7C4(2), which was the control with the highest % identity to 7E5(5), 97% (**Figure 8**). The sequences were 369-374 bp, including an intron of 169 bp. This showed differences in intron length between 7E2 and 7E5. Nucleotides differences in these alignments occurred within introns and exons. Within introns, most nucleotide differences (7) as well as a 5 bp gap occurred in the control. There was only one difference within the introns of experimental clones. Within exons, there were 6 positions with nucleotide changes. Clone 7E5(8) had 4 of 6 positions changed in its coding region.

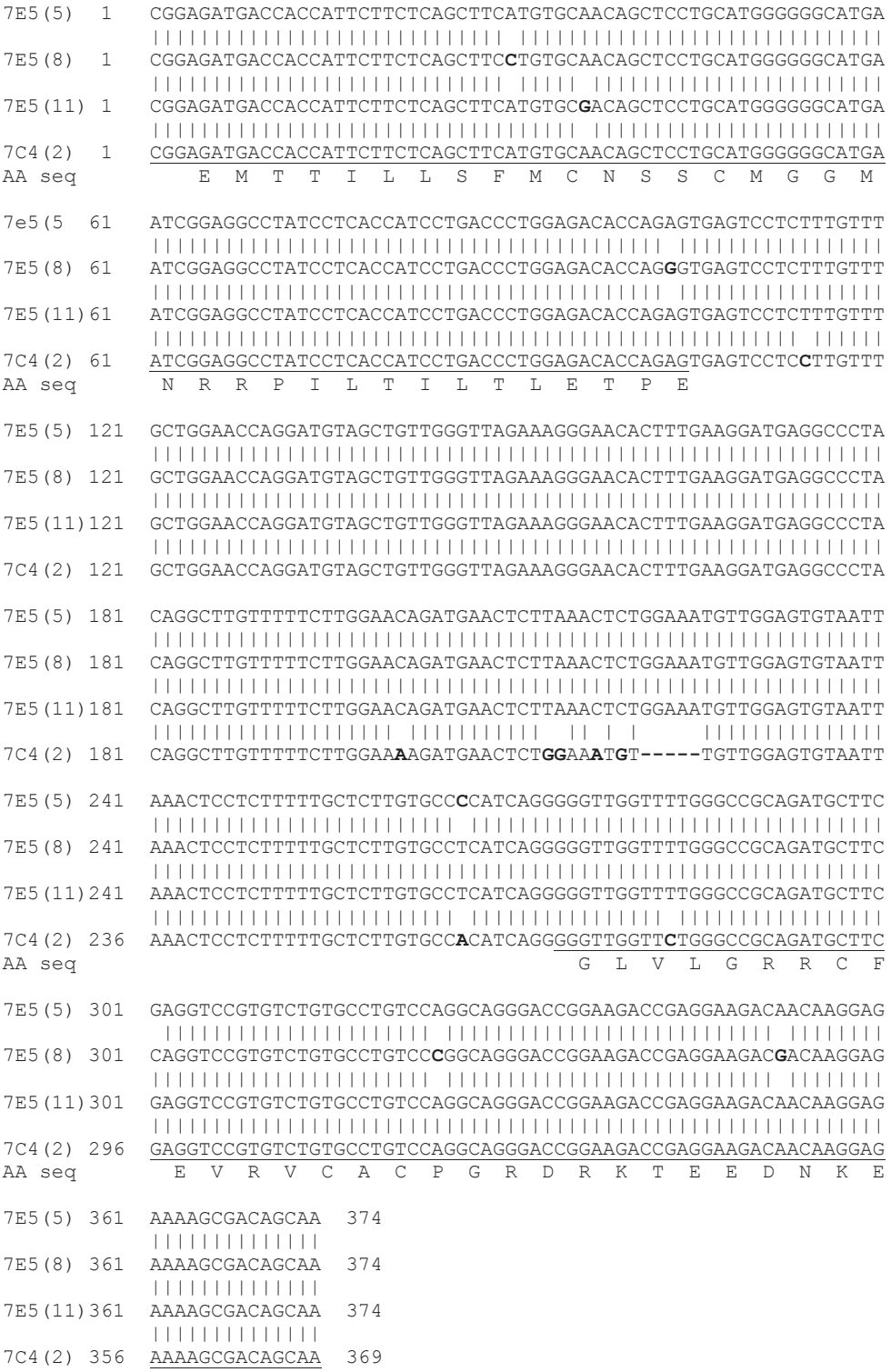

Figure 8: DNA sequences of clones from experimental fish 7E5 and control fish 7C4. Sequences are represented as day of collection – 7 or 7, treatment – E (experimental) or C (Control), fish number – 5 or 4, and clone (number). Variations in nucleotide sequences are boldfaced and the exons are underlined. The amino acid sequence (AA seq) is based on consensus codons.

Clones of 7E14 were aligned to each other and to 3C7(2), which was the control with the highest % identity to 7E14(4), 98% (**Figure 9**). The sequences were 353-355 bp, including an intron of 148 bp. Alignments showed that clones 7E14(4) and 7E14(12) had identical sequences despite the apparent differences in their profiles. Nucleotide differences occurred in introns (9) and exons (3). Most changes occurred in the intron of 7E14(5). Taken together, differences in PCR-SSCP profiles were associated with nucleotide level changes between clones. Most nucleotide changes occurred within introns, but some were found within exons, which could result in altered codons. Clones from 7C4 were also aligned to each other just to show the intron was present in all controls sequenced, and show consensus sequence variations indicated by boldface text (**Figure 10**). All three 7C4 clones show 98% identity with each other.

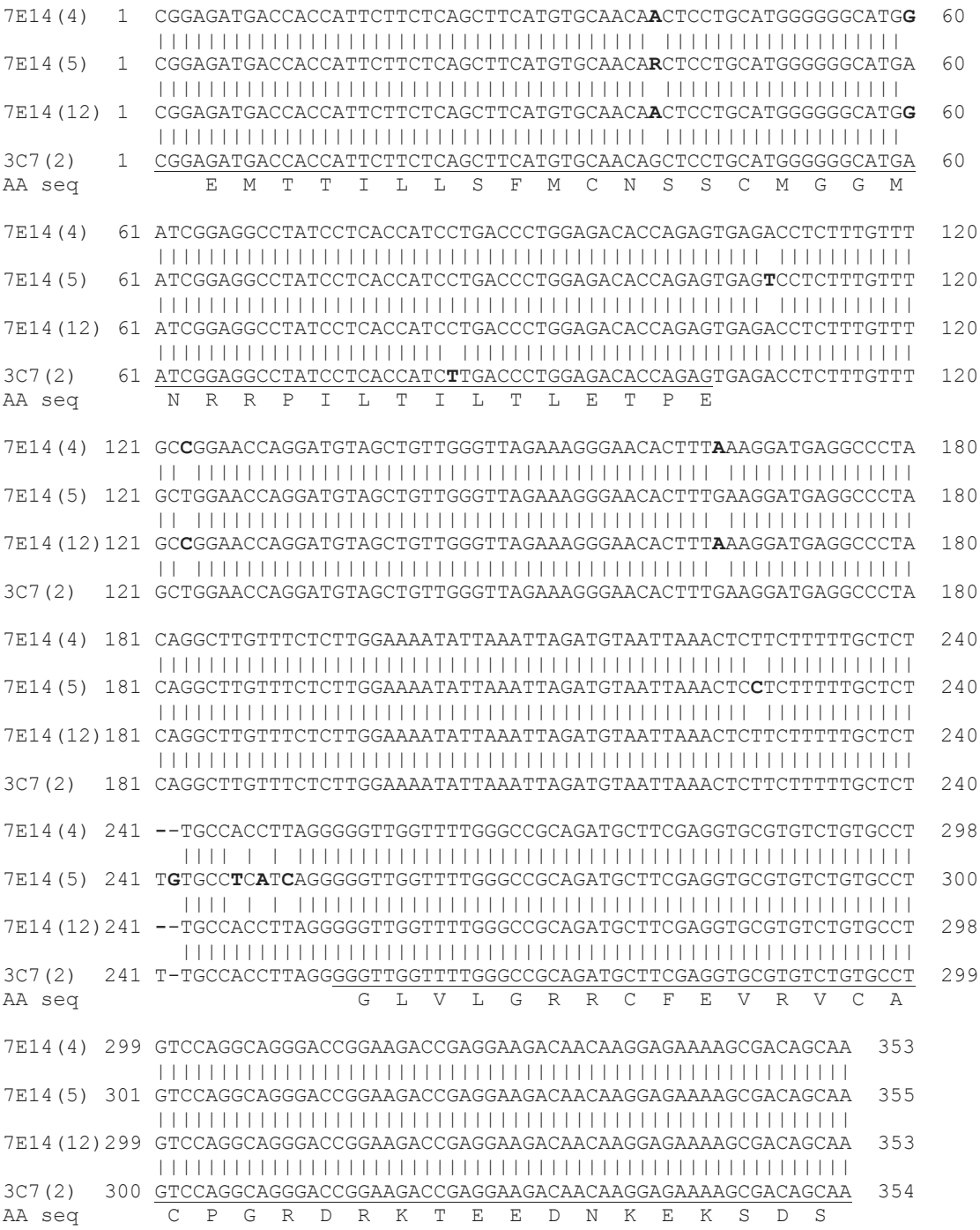

Figure 9: DNA sequences of clones from experimental fish 7E14 and control fish 3C7. Sequences are represented as day of collection – 7 or 3, treatment – E (experimental) or C (Control), fish number – 14 or 7, and clone (number). Variations in nucleotide sequences are boldfaced and the exons are underlined. The amino acid sequence (AA seq) is based on consensus codons.

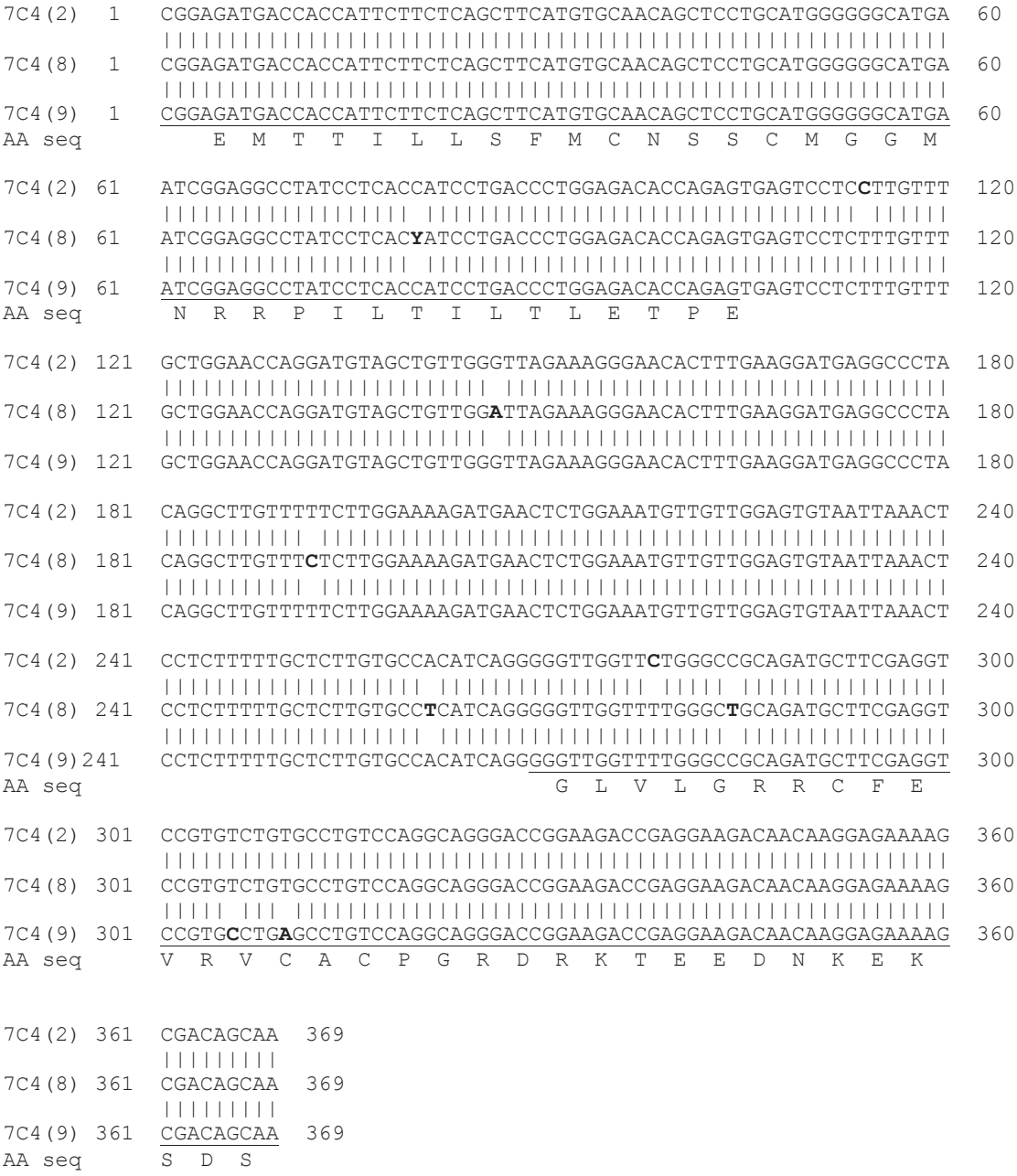

Figure 10: DNA sequences of three clones from experimental fish 7C4. Sequences are represented as day of collection – 7, treatment – C (Control), and fish number – 4, and clone (number). Variations in nucleotide sequences are boldfaced. The amino acid sequence based on the consensus codons is underlined.

All 14 nucleotide sequences were translated into amino acid sequences and aligned to *F. heteroclitus* TP53 X3 (**Figure11**). Alignments of four control clones were 100% identical while a fifth one, 7C4(9), showed three codon changes. One change resulted in a stop codon suggesting that this sequence variant would produce a truncated protein. All 7E2 clones and one 7E5 clone, 7E5(5), also showed no deviation from the original amino acid sequence. However, all remaining experimental clones showed two or three amino acid substitutions. For example, all three clones of 7E14 showed a serine (Ser) to asparagine (Asn) substitution, however this substitution was between two polar amino acids. The most frequently amino acid change was from polar asparagine (Asn) to charged aspartate (Asp). This substitution was identified in 4 of 9 experimental clones, but when evaluating the control clones this substitution was not found.

```
FhX1    EMTTILLSFMCNSSCMGGMNRRPILTILTLETPEGLVLGRRCFEVRVCACPGRDRKTEEDNKEKSDS
0C2(3)  ------------------------------------------------------------------
3C7(2)  ------------------------------------------------------------------
7C4(2)  ------------------------------------------------------------------
7C4(8)  ------------------------------------------------------------------
7C4(9)  ---------------------------------------C------A*-------------------
7E2(6)  ------------------------------------------------------------------
7E2(7)  ------------------------------------------------------------------
7E2(10) ------------------------------------------------------------------
7E5(5)  ------------------------------------------------------------------
7E5(8)  ---------L-----------------------G--------------------------D------
7E5(11) -----------D------------------------------------------------------
7E14(4) ------------N------D---------------------------------------------
7E14(5) ------------N------------------------------------------------------
7E14(12)------------N------D---------------------------------------------

*= stop

7E5(8)  N:Asn (AAC) to D:Asp (GAC)
7E5(11) N:Asn (AAC) to D:Asp (GAC)
7E14(4) N:Asn (AAT) to D:Asp (GAT)
7E14(12)N:Asn (AAT) to D:Asp (GAT)
```

Figure 11. Amino acid sequences of clones from experimental and control fish. Sequences are compared to NCBI *F. heteroclitus* tumor protein *p53* (*tp53*), transcript variant X3, mRNA Accession XM_012874738.1. Dashed lines indicated no change in sequence. Codons associated with conversions of asparagine (Asn) to aspartate (Asp) are provided. Clones are represented as day of collection – 0, 3, or 7, treatment – E (Experimental) or C (Control), fish number, and clone (number). Nucleotide sequences for clones are provided in **Figures 7-10**.

Discussion

Oil spills introduce petrogenic chemicals into environments that would not ordinarily be exposed without human influence. These spills have lasting ramifications on whole ecosystems, and while the effects of acute contamination contact are more familiar, the downstream effects of chronic exposure due to acute dosing are still being investigated. This study aimed to use molecular techniques to evaluate whether the primary toxic components of crude oil, PAHs, are potent enough to cause genotoxicity in an acute exposure. The use of PCR-SSCP aimed to evaluate genotoxicity in the killifish *p53* gene and provide a useful methodology for evaluation of polymorphisms in a gene.

Mutations within the genome, particularly those occurring in crucial cell regulatory genes such as proto-oncogenes or tumor suppressor genes, could have potent consequences on the life and health span of the organisms affected. but also could affect the reproductive capacity of that organism and genomes and fitness of the offspring. *Fundulus heteroclitus*, or killifish, were selected as the model toxicological organism due to their tolerance for extreme toxicant exposure as well as their similar behavioral and morphological characteristics between populations in different geographical regions that may or may not have been exposed to toxicants (Whitehead *et. al.*, 2017). The expectation of this study was that wild caught killifish exposed to Macando 252 (MC252) crude oil via gavage would show polymorphisms within the amplified DNA

binding domain of the tumor suppressor *p53* gene due to previous literature supporting the role of PAHs in genotoxicity. This serves as an exploratory methodology that could be applied to environmentally exposed fish or other organisms to evaluate if exposure leads to adverse effects on the genome. A larger study would be required to make assertions of rate or abundance of polymorphism.

The first step in evaluating the effects of PAHs is ensuring specimen exposure. Excitation-emission matrix spectroscopy (EEMS) is an established method of identifying environmental contamination isolates from sediment, groundwater, and seawater (Zhou *et. al.*, 2013). EEMS spectra are specific enough that pure PAHs can be compared to specimens to determine identity of the compound or unique spectra can be correlated to known metabolites of PAHs. Since PAHs are lipophilic, examining the gallbladder of the fish is ideal as PAHs can accumulate in the bile or fish oil derived from ground tissue (Pena *et. al.,* 2015). All 47 fish in the study had bile and oil extracted from gallbladder homogenates to determine the presence of PAHs in the tissue, and **Figure 1** shows examples of typical control and experimentally exposed fish spectra. 3D scans of control fish all showed characteristic spectra with no apparent PAH residues while the 3D scans showed PAH profiles consistent with the presence of PAH parent compounds and metabolites. The control spectra are consistent with albumin protein spectra seen in this method when specimens were collected from pure fish oil (Pena *et. al.,* 2015) or from bile of fish with lower or no toxicant exposure composed primarily of albumin protein residues (Bentivegna *et.al.,* 2016). The first representative experimental spectra shows maximal fluorescence at Ex340/Em380-400 in the Day 3 experimental fish (3E9) which was consistent with the presence of 1-hydroxypyrene and aligned with the 1-hydroxypyrene standard. The Day 7 experimental

fish (7E2) showed maximal fluorescence at Ex260/Em370-380 which was consistent with the presence of 9-phenanthrol. When comparing the Day 3 and Day 7 experimental spectra, the shift in excitation and emission consistent with 1-hydroxypyrene to 9-phenanthrol indicates preferential metabolism of 1-hydroxypyrene-like PAHs over phenanthrol-like PAHs. Metabolites of PAHs can also be detected in tissue and bile samples and support this preferential metabolism of certain PAHs over others, as seen with benzo-[a]-pyrene and its metabolites in bile collected from English sole, *Parophrys vetulus* (Collier and Varanasi, 1991). **Figure 2** shows that fluorescence in our study when normalized by the weight of the individual fish shows a 100x increase associated with PAHs in experimentally exposed fish. This phenomena is supported by literature where phenanthrene levels can correlate with exposure due to the retention of this compound in fatty tissues and bile in juvenile salmonids fed specific PAHs and tested using high-performance liquid chromatography (HPLC) (Meador *et. al.,* 2008).

Evidence of PAH ingestion and metabolism allowed for the continuation to DNA isolation and analysis of the *p53* DNA binding domain using PCR-SSCP. This technique is sensitive enough to detect small mutations where there is a minor enough base change representative of polymorphism within a gene (Glavač and Dean, 1993). The particular region of the *p53* gene selected, the DNA binding domain, is proposed as the most highly mutative region of the gene with implications of possible downstream protein conformational changes that affect the function (Pavletich *et. al.,* 1993). Six key residues within this sequences are noted as the most commonly mutated (Bullock and Ferst 2001), leading to our interest in its polymorphic profile since certain PAH compounds are noted as possibly genotoxic due to their ability to form adduct structures within genomic DNA. Single point mutations where one base change occurs can be sufficient to

yield cells with malformed, nonfunctional p53 proteins and p53 protein mutations are noted in half of all human cancers (Bullock and Ferst 2001). While typically evaluated in humans due to long life expectancy, exposure to a toxicant that is suspected to yield mutated p53 could be used to model the transition from genotoxicity to tumorigensis in a longer-lived fish species.

Loss of the p53 dependent apoptotic pathway can lead to unregulated growth of mutated cells and be associated with neoplasm, cancer, and metastasis due to the normal protein's role as a tumor suppressor (Freed-Pastor and Prives, 2012). The metabolism of PAHs is significant in possible genotoxicity since the diol-epoxide enantiomers formed as can covalently bond to genomic DNA forming bulky adduct structures, which can lead to point mutations and overall genomic instability (Muñoz and Albores, 2011). **Figure 5** shows the PCR-SSCP banding patterns of all 47 fish and variation is seen across all samples, control and experimental. **Table 5** collates those various profiles into eight individual profiles and quantifies the number seen across all samples where it can be noted that while control samples have varied profiles, two unique profiles are seen in five Day 7 experimental fish, and Day 7 experimental fish had the highest incidence of varied profiles despite the small overall sample size. This suggests that exposure could be correlated with the novel profiles seen in the Day 7 fish and led to our selection of specimens of interest to clone. **Figure 6** shows the selected PCR-SSCP specimens that were cloned and the PCR-SSCP profiles of 15 randomly selected clones from each. An unexpected discovery of sub-profiles, or unique SSCP profiles that differed from the original sequence, suggested the possibility that the liver tissue of one fish could have a dominant SSCP profile where it could be hypothesized that small point mutations could be seen in certain clones and suggest that mutations could be seen further in some of the cells of the tissue or in other

rapidly overturning tissues that were not studied. However, polymorphisms do not always beget loss of protein functionality and it would need to be evaluated further if these specific polymorphisms are associated with loss of function that a mutation would imply. Fifteen clones from each liver DNA sample of the six specimens selected appeared to be sufficient to detect minor sequence changes in what could have been isolated groups of mutated cells that were not detected in the PCR-SSCP of the DNA from the whole liver because initially the dominant profile masked them. Visual profile variation alone was not sufficient to say the sequence had changed despite previous data suggesting that differences in SSCP profile are caused by minor sequence mutations in small DNA fragments (Sheffield *et. al.*, 1993), so boxed sequences in **Figure 6** were sent out for sequencing and the resulting consensus sequences were aligned and evaluated for point mutations.

The original amplicon for the gene of interest in this study was intended to be 205 base pairs as noted in **Table 2**, but as PCR-SSCP samples were run through gels, they consistently showed an amplicon of approximately 260-300 base pairs. The primers were designed based off a RNA transcript variant and applied to genomic DNA, and the initial observation from sequencing was that when comparing consensus sequence to the original RNA transcript, the gene for the DNA binding domain in *p53* is composed of two exons with an intron in between them. The presences of an intron of approximately 150 base pairs was a novel find and ended up being the site of several of the point mutations responsible for possible polymorphic profiles as seen in **Figures 5, 6, and 7**. Intron mutations are typically spliced out, however have been shown in plants to effect the ability to recognize mRNA splice locations leading to incorrect or incomplete splicing (Simpson *et. al.*, 1996). Splicing efficacy due to intron mutations can be reduced or lead to

incorrect gene to protein expression. Sequenced experimental clones were aligned with similar control clones to determine if similar polymorphic SSCP profiles indicated similar nucleotide sequences. Specific point mutations observed in the clone sequences occurred most frequently in the intron regions of the gene, however there were identified point mutations within the exon coding sequence; clones of 7E5 showed five point mutations, 3 in the first exon two in the second, and 7E14 showed two point mutations both in the first exon. Without further evaluation of protein function, it can not be determined if these coding sequence mutations have an effect on the protein structure, but in **Figure 11** the coding sequence of the two exons are translated and spliced together with the point mutations seen in certain clones applied to alter the translated amino acid sequence.

In the aligned amino acid sequences in **Figure 11**, one of the five unique control clones (7C4 clone 9) showed introduction of two amino acid changes, the second of which was the addition of a stop codon that would lead to a truncated protein in a control fish, possibly due to inheritance or environmental exposure to some unknown genotoxic compound. Five of the nine unique experimental clones showed point mutations leading to amino acid sequence changes. Three of the four unchanged clones originated from clones of 7E2 which had a P1 PCR-SSCP profile which was the most common profile seen across all specimens, control and experimental. This is theorized to be the native DNA sequence for the DNA binding domain of the *p53* tumor suppressor gene as it has no exon deviations from the RNA transcript used to design the original primers and was most common or conserved in the sample population. The last unchanged clone was 7E5 clone 5 which is identified as a P2 PCR-SSCP profile in **Figure 4**, which was the second most commonly identified variant profile, indicating likely variation on the commonly

seen P1 gene sequence.

A paper on Japanese flounder, *Paralichthys olivaceus*, linked polymorphisms within the estrogen receptor β (ERβ) coding region to alterations in expression of estrogen in serum and gonadal tissue. While the alternations in the coding sequences seen in the five experimental fish shown in **Figure 11** cannot be directly attributed to downstream effects, there are four sites in five of the experimental fish where asparagine (Asn) residues are mutated to code for aspartic acid (Asp) residues. In all four cases, this amino acid change is due to a transition mutation where an adenine has been replaced by a guanine, though two of the clones, 7E14 clone 4 and 7E14 clone 12 show an identical mutation pattern. This amino acid substitution could change the protein folding structure as the charge of these two amino acids differs and structural integrity of the DNA binding domain is essential to retained function of the p53 protein to scan DNA for damage (Bullock and Ferst, 2001). This specific amino acid transition has been noted before using this same methodology as a mutation associated with bladder cancer in humans (Philips *et. al.*, 2000), however the urinary bladders of these fish were not specifically evaluated for signs of neoplasm. Another mechanism of detection of polymorphisms is PCR followed by restriction fragment length polymorphism (RFLP) analysis where specific restriction sites can be identified when point mutations interfere with enzyme binding. The nucleic acid changes seen in this study were also adenine to guanine transitions seen in European flounder, *Platichthys flesus*, in response to benzo-[a]-pyrene exposure and examination via PCR-RFLP that were identified as they interfered with the *Taq1* restriction site, TCGA (Sueiro *et. al.,* 2000). The identification of mutation and subsequent malignancy associated with mutation in this region suggests that the downstream effects of mutation in the DNA binding domain of *p53* alters the function of the

protein and could lead to neoplasm, although identification of malignancy is typically unlikely in short-lived fish species and was not evaluated in this study.

Genomic variation in wild populations provide resiliency to environmental stressors but may also serve as biomarkers of genotoxicity (Belfiore and Anderson, 2001). In a wild caught population exposed to a toxicant in a laboratory environment, it can be difficult to parse apart whether variations in PCR-SSCP profiles are due to population dynamics and previous exposure or from dosing with crude oil. In the study presented, a modification of the PCR-SSCP technique that involves cloning of PCR amplicons, re-amplification of the amplicon of interest, and re-subjection to SSCP is suggested to evaluate presence of sub-profiles. These sub-profiles are noted as clones presenting with nucleotide substitutions differing from the original profile's sequence. Analysis of DNA sequences from these clones showed greater conservation of exons than introns in the DNA binding region of the p53 gene of wild killifish, which is an expected finding based on current evolutionary genetics (Betts *et. al.,* 2001). However the presence of this intron is proposed as a novel find of this study. This study also suggested that acute crude oil exposure was associated with transition from Asn to Asp codons in the small population evaluated. Asparagine to aspartic acid mutations are associated with genetic disease in other organisms, such as humans, where this specific mutation was found in patients with stage four bladder cancer (Phillips *et.al.,* 2000). Occurrence of this transition in a functionally important region of the P53 protein might link acute crude oil exposure with the possibility of tumorigenesis in fish. However, it remains to be determined if transition from the Asn to Asp codon seen in this study is due to the acute crude oil exposure or present intrinsically in the wild population. Further study would be needed to determine if this is a significant change that

affects protein structure in this model organism, as well as if these polymorphisms are associated with neoplasm in longer-lived fish species or in a larger sample size.

References

Aas E, Baussant T, Balk L, Liewenborg B, Andersen OK. (2000). "PAH metabolites in bile, cytochrome P4501A and DNA adducts as environmental risk parameters for chronic oil exposure: a laboratory experiment with Atlantic cod." Aquat Toxicol. 51(2): 241–258.

Abdel-Banat BM, Koga D. (2002). "Alternative splicing of the primary transcript generates heterogeneity within the products of the gene for *Bombyx mori* chitinase." J Biol. Chem. 277(34): 30524-34.

Adams A. (2015). "Summary of Information concerning the Ecological and Economic Impacts of the BP *Deepwater Horizon* Oil Spill Disaster." NRDC. 15-04-a: 1-9.

Ali AO, Hohn C, Allen PJ, Ford L, Dail MB, Pruett S, Petrie-Hanson L. (2014). "The effects of oil exposure on peripheral blood leukocytes and splenic melano-macrophage centers of Gulf of Mexico fishes." Mar Pollut Bull 79(1-2): 87-93.

Altschul SF, Gish W, Miller W, Myers EW, Lipman DJ. (1990). "Basic local alignment search tool." J. Mol. Biol. 215: 403-10.

Arcand-Hoy L, Metcalfe CD. (1999). "Biomarkers of exposure of brown bullheads (*Ameiurus nebulosus*) to contaminants in the lower Great Lakes, North American." Environ Toxicol Chem. 18(4): 740–749.

Baumann PC, Harshbarger JC. (1998). "Long term trends in liver neoplasm epizootics of Brown Bullhead in the Black River, Ohio." Environ Monitoring and Assessment 53(1): 213-233.

Bailey GS, Williams DE, Hendricks JD. (1996). "Fish models for environmental carcinogenesis: The rainbow trout." Environ Health Perspect. Suppl. 1:5–21.

Benson DA, Karsch-Mizrachi I, Lipman DJ, Ostell J, Wheeler DL. (2005). "GenBank." Nucleic Acids Research 33(Database Issue): 34-38.

Bentivegna CS, DeFelice CR, Murphy WR. (2016). "Excitation-Emission Matrix Scan Analysis of Raw Fish Oil from Coastal New Jersey Menhaden Collected Before and After SuperStorm Sandy. " Marine Pollution Bulletin 107: 442-452.

Betts MJ, Guigó R, Agarwal P, Russell RB. (2001). "Exon structure conservation despite low sequence similarity: a relic of dramatic events in evolution?" EMBO J 20(19): 5354-5360.

Beyer J, Johsson G, Porte C, Krahn MM, Ariese F. (2010). "Analytical methods for determining metabolites of polycyclic aromatic hydrocarbon (PAH) pollutants in fish bile: a review." Environ Toxicol Pharm. 30(3):224-244.

Bugel SM, White LA, Cooper KR. (2010). "Impaired reproductive health of killifish (*Fundulus heteroclitus*) inhabiting Newark Bay, NJ, a chronically contaminated estuary." Aquatic Toxicol 96(3): 182-193.

Bullock AN, Fersht AR. (2001). "Rescuing the function of mutant *p53*." Nat. Rev. Cancer 1: 68-76.

Chomczynski P. (1993). "A regent for the single-step simultaneous isolations of RNA, DNA, and proteins from cell and tissues samples." Biotechniques 15(3): 532-4, 536-7.

Collier TK, Varanasi U. (1991). "Hepatic Activities of Xenobiotic Metabolizing Enzymes and Biliary Levels of Xenobiotics in English Sole (*Parophrys vetulus*) Exposed to Environmental Contaminants." Arch. Environ. Contam. Toxicol. 20 (4): 462-473.

Duvernell DD, Lindmeier JB, Faust KE, Whitehead A. (2008). "Relative influences of historical and contemporary forces shaping the distribution of genetic variation in the Atlantic killifish, *Fundulus heteroclitus*." Molecular Ecology17: 1344–1360.

Ferretto N, Tedetti M, Goutx M, Guigue C, Mounier S, Redon R. (2014). "Identification and quantification of known polycyclic aromatic hydrocarbons and pesticides in complex mixtures using fluorescence excitation–emission matrices and parallel factor analysis." Chemosphere 107: 344–353.

Finn RD, Coggill P, Eberhardt RY, Eddy SR, Mistry J, Mitchell AL, Potter SC, Punta M, Qureshi M, Sangrador-Vegas A, Salazar GA, Tate J, Bateman A. (2016). "The Pfam protein families database: towards a more sustainable future." Nucleic Acids Res 44(Database Issue): 279-285.

Freed-Pastor WA, Prives C. (2012). "Mutant *p53*: One name, many proteins." Genes & Development 26: 1268–1286.

Geacintov NE, Cosman M, Hinerty BE, Amin S, Broyde S, Patel DJ. (1997). "NMR solution structure of stereoisomeric covalent polycyclic aromatic carcinogen-DNA adducts: principles, patterns, and diversity." Chem Res Toxicol 10 (2): 111-146.

Glavač D, Dean M. (1993). "Optimization of the single-strand conformation polymorphism (SSCP) technique for detection of point mutations." Hum. Mutat. 2: 404-414.

Glazko GV, Koonin EV, Rogozin IV. (2004). "Mutation hotspots in the *p53* gene in tumors of different origin: correlation with evolutionary conservation and signs of positive selection. Biochim Biophys Acta 1679(2): 95-106.

Harvey JS, Lyons BP, Page TS, Stewart C, Parry JM. (1999). "An assessment of the genotoxic impact of the Sea Empress oil spill by the measurement of DNA adduct levels in selected invertebrate and vertebrate species." Mutat Res. 441(1): 103–114.

Haupt S, Raghu D, Haupt Y. (2016). "Mutant *p53* Drives Cancer by Subverting Multiple Tumor Suppression Pathways." Front. Oncol. 6: 12-16.

Irvine GV, Mann DH, Short JW. (2006). " Persistence of 10-year old *Exxon Valdez* oil on Gulf of Alaska beaches: The importance of boulder-armoring." Mar Pollution Bulletin 52: 1011-1022.

J**ewett SC, Dean TA, Woodin BR, Hoberg MK, Stegeman JJ.** (2002). "Exposure to hydrocarbons 10 years after the *Exxon Valdez* oil spill: evidence from cytochrome P4501A expression and biliary FACs in nearshore demersal fishes." Mar Environ Res. 54(1): 21–48.

Jung JH, Kim MK, Yim UH, Ha SY, An JG, Won JH, Han GM, Kim NS, Addison RF, Shim WJ. (2011). "Biomarker responses in pelagic and benthic fish over 1 year following the *Hebei Spirit* oil spill (Taean, Korea)." Mar Pollut Bull. 62(8): 1859–1866.

Kamp WM, Wang P, Hwang PM. (2016). "*TP53* Mutation, Mitochondira and Cancer." Curr Opin Genet Dev. 38: 16–22.

Meador JP, Buzitis J, Bravo CF. (2008). "Using fluorescent aromatic compounds in bile from juvenile salmonids to predict exposure to polycyclic aromatic hydrocarbons." Environ. Toxicol. Chem. 27(4): 845–853.

Mukherjee JJ, Gupta SK, Kumar S, Sikka HC. (2004). "Effects of cadmium(II) on (+/-)-anti-benzo[a]pyrene-7,8-diol-9,10-epoxide-induced DNA damage response in human fibroblasts and DNA repair: a possible mechanism of cadmium's cogenotoxicity." Chem Res Toxicol.17(3): 287-293.

Muñoz B, Albores A. (2011). "DNA damage caused by polycyclic aromatic hydrocarbons: mechanisms and markers. Selected Topics in DNA Repair 1: (125-144).

Olson GM, Meyer BM, Portier RJ. (2016). "Assessment of the toxic potential of polycyclic aromatic hydrocarbons (PAHs) affecting Gulf menhaden (*Brevoortia patronus*) harvested from waters impacted by the BP *Deepwater Horizon* Spill." Chemosphere 145: 322-328.

Orita M, Iwahana H, Kanazawa H, Hayashi K, Sekiya T. (1989). "Detection of polymorphism of human DNA by gel electrophoresis as single-strand conformation polymorphisms." Proc. Natl. Acad. Sci 86: 2766-2770.

Pampanin DM, Sydnes MO. (2013). "Polycyclic aromatic hydrocarbons a constituent of petroleum: presence and influence in the aquatic environment." Hydrocarbon. InTech 83-118.

Pavletich NP, Chambers KA, Pabo CO. (1993). "The DNA-binding domain of *p53* contains the four conserved regions and the major mutation hotspots." Genes Dev. 7(12B): 2556-2564.

Pérez-Cadahía B, Méndez J, Pásaro E, Lafuente A, Cabaleiro T, Laffon B. (2008). "Biomonitoring of Human Exposure to Prestige Oil: Effects on DNA and Endocrine Parameters." Environ Health Insights 2: 83-92.

Pena EA, Ridley LM, Murphy WR, Sowa JR, Bentivegna CS. (2015). "Detection of polycyclic aromatic hydrocarbons (PAHs) in raw menhaden fish oil using fluorescence spectroscopy: Method development." Environ Toxicol Chem 34(9): 1946-1958.

Phillips HA, Howard GCW, Miller WR. (2000). "*p53* mutations as a marker of malignancy in bladder washing samples from patients with bladder cancer." Brit J Cancer 82: 136-141.

Pinkney AE, Harshbarger JC, May EB, Reichert WL. (2004). "Tumor prevalence and biomarkers of exposure and response in brown bullhead (*Ameiurus nebulosus*) from the Anacostia River, Washington, DC and Tuckahoe River, Maryland, USA." Environ Toxicol Chem 23(3): 638-647.

Quinn AM, Harvey RG, Penning TM. (2008). "Oxidation of PAH *trans*-Dihydrodiols by Human Aldo-Keto reductase AKR1B10." Chem Res Toxicol. 21: 2207-2215.

Rana SB, Zadlock FJ, Zhang Z, Murphy WR, Bentivegna CS. (2016). "Comparison of *de novo* transcriptome assemblers and *k-mer* strategies using the killifish, *Fundulus heteroclitus*." PLOS ONE 11(4): e0153104.

Roy NK, Stabile J, Seeb JE, Habichit C, Wirgin I. (1999). "High frequency of K-*ras* mutations in pink salmon embryos experimentally exposed to *Exxon valdez* oil." Environ Toxicol Chem. 18(7): 1521-1528.

Sheffield VC, Beck JS, Kwitek AE, Sandstrom DW, Stone EM. (1993). "The sensitivity of single-strand conformation polymorphism analysis for the detection of single base substitutions." Genomics 16 (2): 325-332.

Shi B, Wen HS, He F, Dong SL, Chen CF, Chen XY, Ren J, Zhang Jin JX. (2009). "Single nucleotide polymorphisms within the estrogen receptor beta gene are linked with reproductive indices in Japanese flounder, *Paralichthys olivaceus*." Comp Biochem Physiol B Biochem Mol Biol 154: 62-67.

Short JW, Lindeberg MR, Harris PM, Maselko JM, Pella JJ, Rice, SD. (2003). "Estimate of Oil Persisting on the Beaches of Prince William Sound 12 Years after the *Exxon Valdez* Oil Spill." Environ Science Tech 38: 19-25.

Simpson CG, Clark G, Davidson D, Smith P, Brown JW. (1996). "Mutation of putative branchpoint consensus sequences in plant introns reduces splicing efficiency." Plant J 9(3): 369-380.

Skarphédinsdóttir H, Ericson G, Svavarsson J, Naes K. (2007). "DNA adducts and polycyclic aromatic hydrocarbons (PAH) tissue levels in blue mussels (*Mytilus spp.*) from Nordic coastal sites." Mar Environ Res 64(4): 479-491.

Sueiro RA, Jenkins GJ, Lyons BP, Harvey JS, Parry JM. (2000). "Genotypic mutation analysis in the p53 gene of benzo[a]pyrene-treated European flounder (*Platichthys flesus*)." Mutat Res. 468: 63-71.

Teo SLH, Able KW. (2003). "Habitat use and movement of the mummichog (*Fundulus heteroclitus*) in a restored salt marsh." Estuaries 26: 720-730.

Untergasser A, Cutcutache I, Koressaar T, Ye J, Faircloth BC, Remm M, Rozen SG. (2012). "Primer3--new capabilities and interfaces." Nucleic Acids Res 40(15): e115.

Varanasi U, Reichert WL, Eberhart BTL, Stein JE. (1989). "Formation and persistence of benzo(a)pyrene-diolepoxide-DNA adducts in liver of English sole (*Parophrys vetulus*)." Chem. Biol Interact. 69: 203e216.

Whitehead A, Clark BW, Reid NM, Hahn ME, Nacci D. (2017). "When evolution is the solution to pollution: Key principles, and lessons from rapid repeated adaptation of killifish (*Fundulus heteroclitus*) populations." Evolutionary Applications 7:1-22.

Whitehead A, Dubansky B, Bodinier C, Garcia TI, Miles S, Pilley C. (2011). "Genomic and physiological footprint of the Deepwater Horizon oil spill on resident marsh fishes." Proc Natl Acad Sci 109: 20298–20302.

Zadlock FJ. (2017). " Transcriptome approach for identifying potential biomarkers for endocrine disruption due to crude oil exposure using killifish (Fundulus heteroclitus)." Seton Hall University Dissertations and Theses (ETDs). Paper 2263.

Zhou Z, Guo L, Shiller AM, Lohrenz SE, Asper VL, Osburn CL. (2013). "Characterization of oil components from the Deepwater Horizon oil spill in the Gulf of Mexico using fluorescence EEM and PARAFAC techniques." Marine Chem. 148: 10-21.